ENTROPY CONSERVATIVE AND ENTROPY STABLE SCHEMES FOR NONCONSERVATIVE HYPERBOLIC SYSTEMS[*]

MANUEL J. CASTRO[†], ULRIK S. FJORDHOLM[‡], SIDDHARTHA MISHRA[§], AND CARLOS PARÉS[†]

Abstract. The vanishing viscosity limit of nonconservative hyperbolic systems depends heavily on the specific form of the viscosity. Numerical approximations, such as the path consistent schemes of [C. Parés, *SIAM J. Numer. Anal.,* 41 (2007), pp. 169–185], may not converge to the physically relevant solutions of the system. We construct entropy stable path consistent (ESPC) schemes to approximate nonconservative hyperbolic systems by combining entropy conservative discretizations with numerical diffusion operators that are based on the underlying viscous operator. Numerical experiments for the coupled Burgers system and the two-layer shallow water equations demonstrating the robustness of ESPC schemes are presented.

Key words. nonconservative hyperbolic systems, entropy conservative schemes, entropy stable scheme, two-layer shallow water system

AMS subject classifications. 65M06, 65M08, 76M12

DOI. 10.1137/110845379

1. Introduction. Many problems in science and engineering can be modeled in terms of the first-order quasi-linear system

$$(1.1) \qquad \mathbf{w}_t + A(\mathbf{w})\,\mathbf{w}_x = 0, \quad x \in \mathbb{R},\ t > 0.$$

Here, the unknown $\mathbf{w}(x,t)$ takes values in an open convex set Ω of $\mathbb{R}^N$, and $A \in \mathbb{R}^{N \times N}$ is a smooth locally bounded map. We further assume that the system (1.1) is strictly hyperbolic and that the characteristic fields are either genuinely nonlinear or linearly degenerate.

If there exists a flux vector $\mathbf{f}(\mathbf{w})$ such that $A(\mathbf{w}) = \nabla \mathbf{f}(\mathbf{w})$, then the system (1.1) reduces to a system of *conservation laws*:

$$(1.2) \qquad \mathbf{w}_t + \mathbf{f}(\mathbf{w})_x = 0.$$

It is well known that solutions of nonlinear conservation laws develop discontinuities in finite time, in the form of shock waves. Therefore, solutions of such systems are sought in the sense of distributions. However, in many interesting models in physics, the system (1.1) *cannot* be written in the conservative form (1.2). Examples are the multilayer shallow water systems, multiphase flows, and systems of balance laws.

As shocks are ubiquitous for quasi-linear systems like (1.1), the main mathematical difficulty associated with such *nonconservative* equations is to define the weak solutions. Hence, the nonconservative product $A(\mathbf{w})\mathbf{w}_x$ cannot be defined in the

---

[†]Departamento de Análisis Matemático, Facultad de Ciencias, University of Málaga, 29071 Málaga, Spain (castro@anamat.cie.uma.es, pares@anamat.cie.uma.es).

[‡]Seminar for Applied Mathematics, ETH Zurich, HG J48, 8092 Zürich, Switzerland (ulrikf@sam.math.ethz.ch).

[§]Seminar for Applied Mathematics, ETH Zurich, HG G57.2, 8092 Zürich, Switzerland (smishra@sam.math.ethz.ch).

distributional sense. Nevertheless, under some hypotheses of regularity for $\mathbf{w}$, these products can be defined as Borel measures. The theory introduced by Dal Maso, LeFloch, and Murat [5] allows one to define the nonconservative product $A(\mathbf{w})\,\mathbf{w}_x$ as a bounded measure for functions $\mathbf{w}$ with bounded variation, provided a family of Lipschitz continuous paths $\Phi : [0,1] \times \Omega \times \Omega \to \Omega$ is prescribed, which must satisfy certain regularity and compatibility conditions, in particular

$$(1.3) \qquad \Phi(0; \mathbf{w}_-, \mathbf{w}_+) = \mathbf{w}_-, \qquad \Phi(1; \mathbf{w}_-, \mathbf{w}_+) = \mathbf{w}_+, \qquad \Phi(s; \mathbf{w}, \mathbf{w}) = \mathbf{w}.$$

The interested reader is referred to [5] for a rigorous and complete presentation.

Once the nonconservative product has been defined, one may define the weak solutions of (1.1). According to this theory, across a discontinuity a weak solution has to satisfy the generalized Rankine–Hugoniot condition

$$(1.4) \qquad \sigma[\![\mathbf{w}]\!] = \int_0^1 A(\Phi(s; \mathbf{w}_-, \mathbf{w}_+))\partial_s \Phi(s; \mathbf{w}_-, \mathbf{w}_+)\,ds,$$

where σ is the speed of propagation of the discontinuity, $\mathbf{w}_-$ and $\mathbf{w}_+$ are the left and right limits of the solution at the discontinuity, and $[\![\mathbf{w}]\!] = \mathbf{w}_+ - \mathbf{w}_-$. Notice that if $A(\mathbf{w})$ is the Jacobian matrix of some function $\mathbf{f}(\mathbf{w})$, then (1.4) reduces to the standard Rankine–Hugoniot conditions for the conservation law (1.2), regardless of the chosen family of paths.

Unfortunately, the concept of weak solutions as outlined above depends on the chosen family of paths. Different families of paths lead to different jump conditions, hence different weak solutions. A priori, the choice of paths is arbitrary. Thus, a crucial question is how to choose the "correct" family of paths so as to recover the physically relevant solutions (see [15] and [17] for more details).

In practice, a hyperbolic system like (1.1) is obtained as the limit of a regularized problem when the high-order terms (corresponding to small-scale effects) tend to 0. For instance, it may be the vanishing viscosity limit of a family of parabolic problems:

$$(1.5) \qquad \mathbf{w}_t^\varepsilon + A(\mathbf{w}^\varepsilon)\,\mathbf{w}_x^\varepsilon = \varepsilon(\mathcal{R}(\mathbf{w}^\varepsilon)\mathbf{w}_x^\varepsilon)_x,$$

where the second-order term is elliptic. In this case, the correct jump conditions (corresponding to the physically relevant solutions) should be consistent with the *viscous profiles*, that is, with the traveling wave solutions $\mathbf{w}^\varepsilon(x,t) = V\left(\frac{x-\sigma t}{\varepsilon}\right)$ of (1.5) satisfying $\lim_{\xi\to\pm\infty} V(\xi) = \mathbf{w}_\pm, \lim_{\xi\to\pm\infty} V'(\xi) = 0$. A single-shock solution

$$(1.6) \qquad \mathbf{w}(x,t) = \begin{cases} \mathbf{w}_- & \text{if } x < \sigma t, \\ \mathbf{w}_+ & \text{if } x > \sigma t \end{cases}$$

will be considered admissible if $\mathbf{w} = \lim_{\varepsilon\to 0} \mathbf{w}^\varepsilon$ (almost everywhere).

On the other hand, it can be easily verified that the viscous profile V has to sastisfy the ODE

$$-\sigma V' + \mathcal{A}(V)\,V' = (\mathcal{R}(V)\,V')'.$$

By integrating this ODE over $\xi \in \mathbb{R}$, we obtain the jump condition

$$(1.7) \qquad \sigma[\![\mathbf{w}]\!] = \int_{-\infty}^{\infty} \mathcal{A}(V(\xi))\,V'(\xi)\,d\xi.$$

By comparing this jump condition with (1.4), it seems clear that, in this case, the correct choice for the path connecting the states $\mathbf{w}_-$ and $\mathbf{w}_+$ would be, after a reparameterization, the viscous profile $V(\xi)$.

The main difference from the conservative case (1.2) lies in the fact that every choice of the viscous term $\mathcal{R}$ may lead to a different viscous profile (for the nonconservative system) and consequently to different jump conditions. On the other hand, the Rankine–Hugoniot conditions for the conservative system (1.2) are always recovered independently of the choice of the viscous term. This dependence of the jump conditions, and thus of the definition of weak solutions, on the explicit form of the neglected small-scale effects will have profound implications on the design of efficient numerical methods.

1.1. Numerical methods. Numerical methods for the conservative system (1.2) have undergone intense development in the last decades and are fairly mature now. A very popular paradigm is the conservative finite difference (finite volume) scheme [13]. For simplicity, the spatial domain Ω is divided into uniform intervals $I_i = [x_{j-1/2}, x_{j+1/2}]$ with constant mesh size $\Delta x = x_{j+1/2} - x_{j-1/2}$. A conservative finite difference approximation for (1.2) takes the form

$$(1.8) \qquad \frac{d}{dt}\mathbf{w}_i + \frac{1}{\Delta x}(\mathbf{F}_{i+1/2} - \mathbf{F}_{i-1/2}) = 0,$$

where $\mathbf{w}_i$ approximates either the value $\mathbf{w}(x_i)$ (with $x_i := \frac{x_{i-1/2}+x_{i+1/2}}{2}$) or the cell average of $\mathbf{w}$ in I_i, and

$$\mathbf{F}_{i+1/2}(t) = \mathbf{F}\left(\mathbf{w}_i(t), \mathbf{w}_{i+1}(t)\right)$$

for some consistent numerical flux function $\mathbf{F}$. The numerical fluxes are evaluated by (approximately) solving Riemann problems at each cell interface $x_{i+1/2}$. Higher-order spatial accuracy can be obtained either by using nonoscillatory piecewise polynomial reconstructions like TVD, ENO, or WENO or by employing the discontinuous Galerkin method. Time integration is performed using strong-stability preserving Runge–Kutta methods.

In contrast to the conservative case, numerical schemes for the nonconservative system (1.1) are still in early stages of development. Numerical schemes for nonconservative systems can be written in the following *fluctuation* form [18]:

$$(1.9) \qquad \frac{d}{dt}\mathbf{w}_i + \frac{1}{\Delta x}\left(\mathbf{D}^+_{i-1/2} + \mathbf{D}^-_{i+1/2}\right) = 0.$$

Here,

$$(1.10) \qquad \mathbf{D}^{\pm}_{i+1/2}(t) = \mathbf{D}^{\pm}\left(\mathbf{w}_i(t), \mathbf{w}_{i+1}(t)\right)$$

where $\mathbf{D}^{\pm} : \Omega \times \Omega \mapsto \Omega$ are two Lipschitz continuous functions satisfying

$$(1.11a) \qquad \mathbf{D}^{\pm}(\mathbf{w}, \mathbf{w}) = 0.$$

As discussed before, weak solutions of (1.1) require the specification of a family of paths. The path is explicitly introduced into the scheme (1.9) by imposing the condition of *path consistency* [18]:

$$(1.11b) \qquad \mathbf{D}^-(\mathbf{w}_l, \mathbf{w}_r) + \mathbf{D}^+(\mathbf{w}_l, \mathbf{w}_r) = \int_0^1 A(\Phi(s; \mathbf{w}_l, \mathbf{w}_r))\partial_s \Phi(s; \mathbf{w}_l, \mathbf{w}_r)ds.$$

A suitable family of paths needs to be specified in (1.11b) in order to complete the path consistent scheme. According to [18], a numerical scheme (1.9)–(1.10) satisfying (1.11) is said to be *path conservative*.
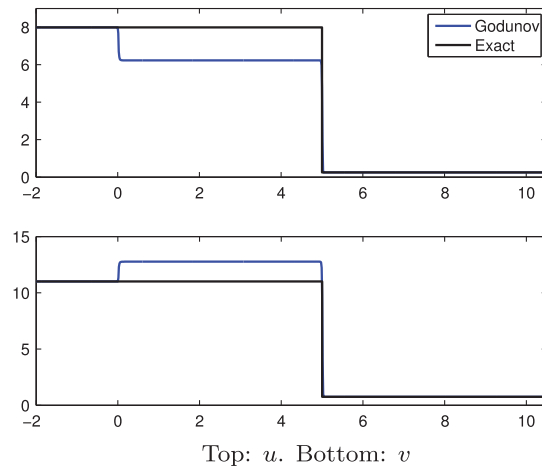
FIG. 1.1. *Godunov method for the coupled Burgers system* (4.1) *with CFL*= 0.4 *and* 1500 *grid points. Comparison with the exact solution computed from the viscous regularization* (4.2).

Assuming that a suitable path is selected (say, by obtaining the corresponding viscous profile), it is natural to investigate whether the approximate solution of (1.1) by the path consistent scheme (1.9) converges to the correct (physically relevant) solution of the nonconservative system (1.1). Unfortunately, the answer to this fundamental question is negative in many cases; see [1], [3], and references therein. We illustrate this deficiency of path consistent schemes by considering a very simple nonconservative system: the coupled Burgers system (4.1). In [2], the viscous profiles corresponding to the parabolic regularization (4.2) have been computed. On the basis of this computation, a Godunov method can be derived by calculating the physically relevant exact solutions of the Riemann problems at the interfaces and averaging these solutions at the next time level under the appropriate CFL condition. Following [16], this Godunov method can also be interpreted as a path consistent scheme. A numerical example (details are provided in section 4) is shown in Figure 1.1. The results show that although the Godunov path consistent scheme converges as the mesh is refined, it *does not* converge to the physically relevant (correct) solution computed explicitly from the corresponding parabolic regularization.

An explanation for this lack of convergence of path consistent schemes lies in the *equivalent equation* of the scheme (1.9):

$$(1.12) \qquad \mathbf{w}_t^{\Delta x} + A(\mathbf{w}^{\Delta x})\,\mathbf{w}_x^{\Delta x} = \Delta x (\widetilde{\mathcal{R}}(\mathbf{w}^{\Delta x})\mathbf{w}_x^{\Delta x})_x + \mathcal{H}.$$

Here, $\mathcal{H}$ includes the higher-order terms that arise from a formal Taylor expansion of the scheme (1.9) and $\widetilde{\mathcal{R}}$ is the (implicit) numerical viscosity. Assuming that the high-order terms are *small* (valid for shocks with small amplitude), we can expect that jump conditions of the numerical solutions to be, at best, consistent with the viscous profiles of the regularized equation

$$(1.13) \qquad \mathbf{w}_t^{\Delta x} + A(\mathbf{w}^{\Delta x})\,\mathbf{w}_x^{\Delta x} = \Delta x (\widetilde{\mathcal{R}}(\mathbf{w}^{\Delta x})\mathbf{w}_x^{\Delta x})_x.$$

In general, $\mathcal{R} \neq \widetilde{\mathcal{R}}$. As discussed before, the solutions of the nonconservative system (1.1) depend *explicitly* on the underlying viscosity operator. Therefore, the numerical solutions generated by the scheme (1.9) may not converge to the physically relevant

solutions of (1.1). Thus, the (implicit) numerical viscosity that is added by any finite difference scheme (see [10]) is responsible for the observed lack of convergence to the physically relevant solution.

The above discussion suggests modifying the numerical viscosity of a finite difference scheme to match the underlying viscous regularization of the system (1.1) as a possible solution to the problem of nonconvergence, at least when the residual terms $\mathcal{H}$ in the equivalent equation (1.12) are small.

In [11], the author calculates the viscous term of the equivalent equation for any scheme and then adds a discretization of the physical viscosity (while subtracting an appropriate discretization of the numerical viscosity). This technique was shown to improve the convergence of the numerical solutions to the correct weak solutions. However, the explicit calculation of the viscous term of the equivalent equation may be quite difficult for complex numerical methods and/or systems.

In this paper, we will design a robust numerical scheme for the nonconservative system (1.1). Our starting point is the concept of *entropy*. We assume that (1.1) is equipped with an entropy pair (η, q), i.e., a convex function $\eta : \Omega \to \mathbb{R}$ and a function $q : \Omega \to \mathbb{R}$ such that $\nabla q(\mathbf{w})^\top = \mathbf{v}^\top A(\mathbf{w})$, where $\mathbf{v} := \nabla \eta(\mathbf{w})$ are the so-called entropy variables. Then smooth solutions of (1.1) satisfy the entropy equality

$$(1.14) \qquad \eta(\mathbf{w})_t + q(\mathbf{w})_x = 0.$$

The first step of our strategy for designing a robust scheme will be to derive a *path consistent* scheme of the form (1.9) that satisfies a discrete version of the entropy identity (1.14). This *entropy conservative path consistent* (ECPC) scheme will generalize the notion of entropy conservative schemes for the conservation law (1.2), proposed by Tadmor [20], to nonconservative hyperbolic systems. The biggest advantage of an entropy conservative discretization lies in the fact that it adds *no* numerical viscosity (up to second order). Hence, $\widetilde{\mathcal{R}} \equiv 0$ in the equivalent equation for an entropy conservative scheme.

As entropy must be dissipated at shocks, we need to add some numerical viscosity to stabilize the entropy conservative scheme. The second step of our approach is to obtain an *entropy stable path consistent* (ESPC) scheme for (1.1) by adding numerical viscosity that matches the underlying physical viscosity in the regularized problem (1.5), thus choosing $\widetilde{\mathcal{R}} = \mathcal{R}$ in the equivalent equation of the scheme. We demonstrate, through several numerical experiments, that our entropy stable scheme approximates the correct (physically relevant) solutions of (1.1) efficiently. We remark that this strategy was also pursued in a recent paper [6] in the context of a model nonconservative system, the equations of Lagrangian gas dynamics.

2. ECPC schemes. In this section, we introduce the notion of ECPC schemes for the nonconservative hyperbolic system (1.1). Recall that given an entropy η, the entropy variables are defined as $\mathbf{v} = \mathbf{v}(\mathbf{w}) := \nabla \eta(\mathbf{w})$.

THEOREM 2.1. *Assume that the nonconservative system* (1.1) *is equipped with an entropy pair* (η, q). *If the fluctuations* $\mathbf{D}^\pm$ *in the finite difference scheme* (1.9) *satisfy*

$$(2.1) \qquad \mathbf{v}_l^\top \mathbf{D}^-(\mathbf{w}_l, \mathbf{w}_r) + \mathbf{v}_r^\top \mathbf{D}^+(\mathbf{w}_l, \mathbf{w}_r) = q(\mathbf{w}_r) - q(\mathbf{w}_l) \qquad \forall\, \mathbf{w}_l, \mathbf{w}_r \in \Omega,$$

then the approximate solutions $\mathbf{w}_i$ *satisfy the discrete entropy identity*

$$(2.2) \qquad \frac{d}{dt}\eta(\mathbf{w}_i) + \frac{1}{\Delta x}(Q_{i+1/2} - Q_{i-1/2}) = 0,$$

where Q is a numerical entropy flux which is consistent with the entropy flux q, that is, $Q(\mathbf{w}, \mathbf{w}) = q(\mathbf{w})$.

Proof. Let us first define

$$
\begin{aligned}
Q_{i+1/2} = Q(\mathbf{w}_i, \mathbf{w}_{i+1}) &= q(\mathbf{w}_i) + \mathbf{v}_i^\top \mathbf{D}^-(\mathbf{w}_i, \mathbf{w}_{i+1}) \\
&= q(\mathbf{w}_{i+1}) - \mathbf{v}_{i+1}^\top \mathbf{D}^+(\mathbf{w}_i, \mathbf{w}_{i+1}),
\end{aligned}
$$

the second equality following from (2.1). Due to (1.11a), one has $Q(\mathbf{w}, \mathbf{w}) = q(\mathbf{w})$, and thus Q is a consistent numerical entropy flux. By multiplying (1.9) by $\mathbf{v}_i = \nabla_{\mathbf{w}} \eta(\mathbf{w}_i)$ we obtain

$$
\begin{aligned}
\frac{d}{dt} \eta(\mathbf{w}_i) &= -\frac{1}{\Delta x} \left(\mathbf{v}_i^\top \mathbf{D}_{i+1/2}^- + \mathbf{v}_i^\top \mathbf{D}_{i-1/2}^+ \right) \\
&= -\frac{1}{\Delta x} \left(\left(\mathbf{v}_i^\top \mathbf{D}_{i+1/2}^- + q(\mathbf{w}_i) \right) - \left(q(\mathbf{w}_i) - \mathbf{v}_i^\top \mathbf{D}_{i-1/2}^+ \right) \right) \\
&= -\frac{1}{\Delta x} \left(Q_{i+1/2} - Q_{i-1/2} \right),
\end{aligned}
$$

resulting in (2.2).   ☐

This leads us to define the following.

DEFINITION 2.2. *Assume that the nonconservative hyperbolic system* (1.1) *is equipped with an entropy pair* (η, q) *and a family of paths* Φ. *A numerical scheme* (1.9) *for this system is said to be ECPC with respect to* (η, q) *and* Φ *if it satisfies*

  (i) *the path consistency condition* (1.11) *and*

  (ii) *the entropy conservation condition* (2.1).   ☐

A priori, it is unclear whether there exists any finite difference scheme that satisfies the discrete entropy conservation condition (2.1) for any choice of path Φ. We show that not only do such schemes exist, there are in fact infinitely many of them for every choice of path.

THEOREM 2.3. *Given any entropy pair* (η, q) *and family of paths* Φ, *there exist infinitely many ECPC schemes.*

Proof. For the sake of notational simplicity, let us drop the dependence on $\mathbf{w}_l$ and $\mathbf{w}_r$ and denote $\Phi(s; \mathbf{w}_l, \mathbf{w}_r) = \Phi(s)$, $\partial_s \Phi(s; \mathbf{w}_l, \mathbf{w}_r) = \Phi'(s)$, and $\mathbf{v}_r - \mathbf{v}_l = [\![v]\!]$. By using the identity $\nabla q(\mathbf{w})^\top = \mathbf{v}^\top A(\mathbf{w})$, the condition (2.1) can be written in the more revealing form

$$
(2.3) \qquad \mathbf{v}_l^\top \mathbf{D}^- + \mathbf{v}_r^\top \mathbf{D}^+ = \int_0^1 \mathbf{v}(\Phi(s))^\top A(\Phi(s)) \Phi'(s) \, ds.
$$

Assume that there exist matrices $B^-(s) = B^-(s; \mathbf{w}_l, \mathbf{w}_r)$ and $B^+(s) = B^+(s; \mathbf{w}^-, \mathbf{w}^+)$ such that

$$
\begin{aligned}
B^-(s) + B^+(s) &= I, \\
B^-(s)\mathbf{v}_l + B^+(s)\mathbf{v}_r &= \mathbf{v}(\Phi(s)).
\end{aligned}
$$

Then it can easily be checked that

$$
\begin{aligned}
\mathbf{D}^- &= \int_0^1 B^-(s)^\top A(\Phi(s)) \Phi'(s) \, ds, \\
\mathbf{D}^+ &= \int_0^1 B^+(s)^\top A(\Phi(s)) \Phi'(s) \, ds
\end{aligned}
$$

satisfies (1.11a), (1.11b), (2.3). If we take $B^-(s) = I - B^+(s)$, then the matrix $B^+(s)$ would need to satisfy $B^+(s)[\![\mathbf{v}]\!] = (\mathbf{v}(\Phi(s)) - \mathbf{v}_l)$. The most obvious choice is

$$B^+(s) = \frac{1}{|[\![\mathbf{v}]\!]|^2}\left(\mathbf{v}(\Phi(s)) - \mathbf{v}_l\right)[\![\mathbf{v}]\!]^\top,$$

where $|[\![\mathbf{v}]\!]|$ denotes the Euclidean norm of the vector $[\![\mathbf{v}]\!]$. We thus obtain

$$\mathbf{D}^- = \int_0^1 \left(I - \frac{1}{|[\![\mathbf{v}]\!]|^2}[\![\mathbf{v}]\!]\left(\mathbf{v}(\Phi(s)) - \mathbf{v}_l\right)^\top\right)A(\Phi(s))\Phi'(s)\,ds,$$

$$\mathbf{D}^+ = \int_0^1 \frac{1}{|[\![\mathbf{v}]\!]|^2}[\![\mathbf{v}]\!]\left(\mathbf{v}(\Phi(s)) - \mathbf{v}_l\right)^\top A(\Phi(s))\Phi'(s)\,ds.$$

Alternatively, one may take $B^+(s) = I - B^-(s)$ and solve for $B^-(s)$. This leads to the different solution

$$\mathbf{D}^- = \int_0^1 \frac{1}{|[\![\mathbf{v}]\!]|^2}[\![\mathbf{v}]\!]\left(\mathbf{v}_r - \mathbf{v}(\Phi(s))\right)^\top A(\Phi(s))\Phi'(s)\,ds,$$

$$\mathbf{D}^+ = \int_0^1 \left(I - \frac{1}{|[\![\mathbf{v}]\!]|^2}[\![\mathbf{v}]\!]\left(\mathbf{v}_r - \mathbf{v}(\Phi(s))\right)^\top\right)A(\Phi(s))\Phi'(s)\,ds.$$

Any convex combination of these two solutions would also give a new solution; for instance, taking the average of the two, we get

$$\mathbf{D}^- = \int_0^1 \left(\frac{1}{2}I - \frac{1}{|[\![\mathbf{v}]\!]|^2}[\![\mathbf{v}]\!]\left(\mathbf{v}(\Phi(s)) - \overline{\mathbf{v}}\right)^\top\right)A(\Phi(s))\Phi'(s)\,ds,$$

$$\mathbf{D}^+ = \int_0^1 \left(\frac{1}{2}I + \frac{1}{|[\![\mathbf{v}]\!]|^2}[\![\mathbf{v}]\!]\left(\mathbf{v}(\Phi(s)) - \overline{\mathbf{v}}\right)^\top\right)A(\Phi(s))\Phi'(s)\,ds,$$

where $\overline{\mathbf{v}} = \frac{\mathbf{v}_l + \mathbf{v}_r}{2}$. Thus, we obtain infinitely many ECPC schemes for any given path Φ.   □

2.1. Systems of conservation laws. The conservation law (1.2) is a special case of (1.1) obtained by setting $A(\mathbf{w}) = \nabla\mathbf{f}(\mathbf{w})$. The notion of entropy conservative schemes for conservation laws was proposed by Tadmor in [20]. Assume that the conservative system (1.2) is equipped with an entropy pair (η, q), that is, a convex function $\eta(\mathbf{w})$ and a function $q(\mathbf{w})$ such that $\nabla q(\mathbf{w})^\top = \mathbf{v}^\top \nabla\mathbf{f}(\mathbf{w})$, where $\mathbf{v} = \nabla\eta(\mathbf{w})$ are the entropy variables. Define also the *entropy potential* $\psi = \mathbf{v}^\top\mathbf{f} - q$. We recall the definition of an entropy conservative scheme for the conservation law (1.2).

DEFINITION 2.4 (Tadmor [20]). *The conservative finite difference scheme* (1.8) *is* entropy conservative *if the numerical flux* $\mathbf{F}$ *satisfies*

$$(2.4) \qquad\qquad [\![\mathbf{v}]\!]^\top \mathbf{F}(\mathbf{u}_l, \mathbf{u}_r) = [\![\psi]\!]. \qquad □$$

It was shown in [20] that solutions computed with an entropy conservative scheme (in the sense of (2.4)) satisfy the entropy equality (2.2). It is natural to require that our notion of ECPC schemes for the nonconservative system reduces to the notion of entropy conservative schemes whenever the system is conservative. This is shown in the following lemma.

LEMMA 2.5. *Assume that* $A(\mathbf{w}) = \nabla\mathbf{f}$ *and let* (1.9) *be an ECPC scheme. Then the scheme* (1.8) *with numerical flux*

$$
\begin{aligned}
(2.5) \qquad \mathbf{F}(\mathbf{w}_l, \mathbf{w}_r) &= \mathbf{f}(\mathbf{w}_l) + \mathbf{D}^-(\mathbf{w}_l, \mathbf{w}_r) \\
&= \mathbf{f}(\mathbf{w}_r) - \mathbf{D}^+(\mathbf{w}_l, \mathbf{w}_r)
\end{aligned}
$$

is equivalent to (1.9) *and is entropy conservative in the sense of* (2.4).

Proof. Note that the second equality in (2.5) follows from (1.11a). By adding and subtracting $\mathbf{f}(\mathbf{w}_i)$ in (1.9) and by taking into account (2.5), it is easily shown that (1.9) is equivalent to (1.8). For entropy conservation, we have

$$
\begin{aligned}
[\![\mathbf{v}]\!]^\top \mathbf{F} &= \mathbf{v}_r^\top \left(\mathbf{f}(\mathbf{w}_r) - \mathbf{D}^+ \right) - \mathbf{v}_l^\top \left(\mathbf{f}(\mathbf{w}_l) + \mathbf{D}^- \right) \\
&= [\![\mathbf{v}^\top \mathbf{f}]\!] - [\![q]\!] \\
&= [\![\psi]\!]
\end{aligned}
$$

so that (2.4) is satisfied. $\qquad\square$

2.2. Systems of balance laws. A balance law

$$
(2.6) \qquad \mathbf{u}_t + \mathbf{f}(\mathbf{u})_x = \mathbf{S}(\mathbf{u}) b_x
$$

for some $b : \mathbb{R} \to \mathbb{R}$ and $\mathbf{S} : \mathbb{R}^n \to \mathbb{R}^n$ is a special case of the nonconservative system (1.1). Writing

$$
(2.7) \qquad \mathbf{w} = \begin{bmatrix} \mathbf{u} \\ b \end{bmatrix}, \qquad A(\mathbf{w}) = \begin{bmatrix} \nabla \mathbf{f}(\mathbf{u}) & -\mathbf{S}(\mathbf{u}) \\ 0 & 0 \end{bmatrix},
$$

we recover the balance law (2.6). We assume that the homogeneous system (when $b \equiv 0$) is equipped with an entropy pair (η, q). In many cases this pair can be extended to obtain an entropy framework for the system of balance laws, that is, there exists a pair $(\tilde{\eta}(\mathbf{w}), \tilde{q}(\mathbf{w}))$ such that $\tilde{\eta}$ is convex and

$$
\nabla_{\mathbf{u}} \tilde{q}(\mathbf{w})^\top = \nabla_{\mathbf{u}} \tilde{\eta}(\mathbf{w})^\top \nabla \mathbf{f}(\mathbf{u}), \quad \partial_b \tilde{q}(\mathbf{w}) = - \left(\nabla \eta(\mathbf{u}) + \nabla_{\mathbf{u}} \tilde{\eta}(\mathbf{w}) \right)^\top \mathbf{S}(\mathbf{u}).
$$

It can easily be checked that $(\eta(\mathbf{u}) + \tilde{\eta}(\mathbf{w}), \ q(\mathbf{u}) + \tilde{q}(\mathbf{w}))$ is an entropy pair for (1.1), (2.7). The following notation will be used for the entropy variables:

$$
\mathbf{v} = \nabla \eta(\mathbf{u}), \quad \tilde{\mathbf{v}} = \nabla_{\mathbf{u}} \tilde{\eta}(\mathbf{w}), \quad \mathbf{V} = \nabla \left(\eta(\mathbf{u}) + \tilde{\eta}(\mathbf{w}) \right).
$$

Let us suppose that a family of paths has been chosen. The following notation will be used:

$$
\Phi(s; \mathbf{w}_l, \mathbf{w}_r) = \begin{bmatrix} \Phi_{\mathbf{u}}(s; \mathbf{w}_l, \mathbf{w}_r) \\ \Phi_b(s; \mathbf{w}_l, \mathbf{w}_r) \end{bmatrix}.
$$

The family of paths is supposed to satisfy the following natural assumption: if two states $\mathbf{w}_l$ and $\mathbf{w}_r$ are such that $b_l = b_r = b$, then $\Phi_b(s; \mathbf{w}_l, \mathbf{w}_r) = b$ for all $s \in [0, 1]$. This property implies that the generalized Rankine–Hugoniot (1.4) reduces to the standard one for jumps evolving in regions where b is continuous: $\sigma[\![\mathbf{u}]\!] = [\![\mathbf{f}(\mathbf{u})]\!]$.

Next, we consider the question of obtaining entropy conservative schemes for balance laws. Let us consider numerical schemes of the form

$$
(2.8) \qquad \frac{d}{dt} \mathbf{u}_i + \frac{1}{\Delta x} \left(\mathbf{F}_{i+1/2} - \mathbf{F}_{i-1/2} \right) = \frac{1}{\Delta x} \left(\mathbf{S}^-_{i+1/2} + \mathbf{S}^+_{i-1/2} \right),
$$

where

$$
\mathbf{F}_{i+1/2} = \mathbf{F}(\mathbf{w}_i, \mathbf{w}_{i+1}), \quad \mathbf{S}^\pm_{i+1/2} = \mathbf{S}^\pm(\mathbf{w}_i, \mathbf{w}_{i+1}),
$$

for some continuous functions $\mathbf{F}, \mathbf{S}^\pm$.

THEOREM 2.6. *If* $\mathbf{F}$ *is a consistent numerical flux satisfying* (2.4) *and* $\mathbf{S}^{\pm}$ *satisfy*

$$
\text{(2.9a)} \qquad\qquad\qquad \mathbf{S}^{\pm}(\mathbf{w}, \mathbf{w}) = 0,
$$

$$
\text{(2.9b)} \qquad \mathbf{S}^{-}(\mathbf{w}_l, \mathbf{w}_r) + \mathbf{S}^{+}(\mathbf{w}_l, \mathbf{w}_r) = \int_0^1 \mathbf{S}(\Phi_{\mathbf{u}}(s; \mathbf{w}_l, \mathbf{w}_r))\partial_s \Phi_b(s; \mathbf{w}_l, \mathbf{w}_r)\, ds,
$$

$$
\text{(2.9c)} \quad \mathbf{V}_l^{\top}\mathbf{S}^{-}(\mathbf{w}_l, \mathbf{w}_r) + \mathbf{V}_r^{\top}\mathbf{S}^{+}(\mathbf{w}_l, \mathbf{w}_r) = [\![\tilde{\mathbf{v}}^{\top}\mathbf{f}]\!] - [\![\tilde{\mathbf{v}}]\!]^{\top}\mathbf{F}(\mathbf{w}_l, \mathbf{w}_r) - [\![\tilde{q}]\!],
$$

then (2.8) *is an ECPC scheme.*

Proof. Let us introduce the following functions:

$$
\text{(2.10)} \qquad\qquad \mathbf{D}^{-}(\mathbf{w}_l, \mathbf{w}_r) = \begin{bmatrix} \mathbf{F}(\mathbf{u}_l, \mathbf{u}_r) - \mathbf{f}(\mathbf{u}_l) - \mathbf{S}^{-}(\mathbf{w}_l, \mathbf{w}_r) \\ 0 \end{bmatrix},
$$

$$
\text{(2.11)} \qquad\qquad \mathbf{D}^{+}(\mathbf{w}_l, \mathbf{w}_r) = \begin{bmatrix} \mathbf{f}(\mathbf{u}_r) - \mathbf{F}(\mathbf{u}_l, \mathbf{u}_r) - \mathbf{S}^{+}(\mathbf{w}_l, \mathbf{w}_r) \\ 0 \end{bmatrix}.
$$

It can easily be checked that the corresponding numerical scheme (1.9) is equivalent to the one given by (2.8) together with

$$
\frac{d}{dt}b_i = 0.
$$

On the other hand, it can easily be checked that (2.9a)–(2.9b) imply (1.11a)–(1.11b). Let us prove finally that (2.1) holds:

$$
\begin{aligned}
\mathbf{V}_l^{\top}&\mathbf{D}^{-}(\mathbf{w}_l, \mathbf{w}_r) + \mathbf{V}_r^{\top}\mathbf{D}^{+}(\mathbf{w}_l, \mathbf{w}_r) \\
&= [\![(\mathbf{v} + \tilde{\mathbf{v}})^{\top}\mathbf{f}]\!] - [\![\mathbf{v} + \tilde{\mathbf{v}}]\!]^{\top}\mathbf{F}(\mathbf{u}_l, \mathbf{u}_r) - \left(\tilde{\mathbf{v}}_l^{\top}\mathbf{S}^{-}(\mathbf{w}_l, \mathbf{w}_r) + \bar{\mathbf{v}}_r^{\top}\mathbf{S}^{+}(\mathbf{w}_l, \mathbf{w}_r)\right) \\
&= [\![\mathbf{v}^{\top}\mathbf{f}]\!] - [\![\psi]\!] + [\![\tilde{\mathbf{v}}^{\top}\mathbf{f}]\!] - [\![\tilde{\mathbf{v}}]\!]^{\top}\mathbf{F}(\mathbf{u}_l, \mathbf{u}_r) - \left(\tilde{\mathbf{v}}_l^{\top}\mathbf{S}^{-}(\mathbf{w}_l, \mathbf{w}_r) + \tilde{\mathbf{v}}_r^{\top}\mathbf{S}^{+}(\mathbf{w}_l, \mathbf{w}_r)\right) \\
&= [\![q + \tilde{q}]\!],
\end{aligned}
$$

where (2.4) and (2.9c) have been used. $\quad\square$

Remark 2.7. The entropy conservative well-balanced schemes for the single layer shallow water system with nontrivial bottom topography, designed in a recent paper [7] and [8], can easily be verified as an example of an ECPC scheme for a system of balance laws, consistent with the family of straight line segments.

3. ESPC schemes. It is well known that the entropy for a nonlinear hyperbolic system like (1.1) should be dissipated at shocks. Consequently, entropy conservative schemes lead to oscillations when shocks are present in the solution. This is already seen in entropy conservative schemes for the conservation law (1.2). Hence, we need to add some numerical viscosity in order to ensure entropy dissipation.

To this end, we consider numerical schemes of the form

$$
\text{(3.1a)} \qquad\qquad \frac{d}{dt}\mathbf{w}_i + \frac{1}{\Delta x}\left(\widetilde{\mathbf{D}}_{i-1/2} + \widetilde{\mathbf{D}}_{i+1/2}\right) = 0,
$$

where $\widetilde{\mathbf{D}}_{i+1/2}^{\pm} = \widetilde{\mathbf{D}}^{\pm}(\mathbf{w}_i, \mathbf{w}_{i+1})$ are defined by

$$
\text{(3.1b)} \qquad\qquad \widetilde{\mathbf{D}}^{+}(\mathbf{w}_i, \mathbf{w}_{i+1}) = \mathbf{D}^{+}(\mathbf{w}_i, \mathbf{w}_{i+1}) + \frac{\varepsilon}{\Delta x}\widehat{\mathcal{R}}(\mathbf{v}_{i+1} - \mathbf{v}_i),
$$

$$
\text{(3.1c)} \qquad\qquad \widetilde{\mathbf{D}}^{-}(\mathbf{w}_i, \mathbf{w}_{i+1}) = \mathbf{D}^{-}(\mathbf{w}_i, \mathbf{w}_{i+1}) - \frac{\varepsilon}{\Delta x}\widehat{\mathcal{R}}(\mathbf{v}_{i+1} - \mathbf{v}_i).
$$

Here, $\mathbf{D}^{\pm}$ are the fluctuations of an ECPC scheme (with respect to some given entropy pair (η, q) and family of paths Φ), and $\widehat{\mathcal{R}} = \widehat{\mathcal{R}}(\mathbf{w}_l, \mathbf{w}_r)$ is a symmetric positive definite matrix. Note that we are adding numerical diffusion in terms of the entropy variables. The properties of the scheme are listed below.

THEOREM 3.1. *The numerical scheme* (3.1)

(i) *is path consistent with respect to* Φ *and*

(ii) *satisfies the discrete entropy inequality*

$$(3.2) \qquad \frac{d}{dt}\eta(\mathbf{w}_i) + \frac{1}{\Delta x}(\widetilde{Q}_{i+1/2} - \widetilde{Q}_{i-1/2}) \leq 0$$

for some numerical entropy flux $\widetilde{Q}$ *that is consistent with* q.

Proof. Property (i) follows from the path consistency of $\mathbf{D}^{\pm}$, as $\widetilde{\mathbf{D}}^{\pm}(\mathbf{w}, \mathbf{w}) = \mathbf{D}^{\pm}(\mathbf{w}, \mathbf{w}) = 0$ and $\widetilde{\mathbf{D}}^{-} + \widetilde{\mathbf{D}}^{+} = \mathbf{D}^{-} + \mathbf{D}^{+}$. To prove (ii), we multiply both sides with $\mathbf{v}_i$ and imitate the calculations in the proof of Theorem 2.1 to obtain the identity

$$\frac{d}{dt}\eta(\mathbf{w}_i) + \frac{1}{\Delta x}(\widetilde{Q}_{i+1/2} - \widetilde{Q}_{i-1/2}) = -\frac{1}{2\Delta x}(\mathbf{v}_{i+1} - \mathbf{v}_i)^{\top}\widehat{\mathcal{R}}(\mathbf{v}_{i+1} - \mathbf{v}_i)$$
$$-\frac{1}{2\Delta x}(\mathbf{v}_i - \mathbf{v}_{i-1})^{\top}\widehat{\mathcal{R}}(\mathbf{v}_i - \mathbf{v}_{i-1})$$

with numerical entropy flux

$$\widetilde{Q}_{i+1/2} = Q(\mathbf{w}_i, \mathbf{w}_{i+1}) = q(\mathbf{w}_i) + \mathbf{v}_i^{\top}\mathbf{D}^{-}(\mathbf{w}_i, \mathbf{w}_{i+1}) - \frac{1}{2}(\mathbf{v}_{i+1} + \mathbf{v}_i)^{\top}\widehat{\mathcal{R}}(\mathbf{v}_{i+1} - \mathbf{v}_i).$$

Clearly $\widetilde{Q}$ is consistent with q. The discrete entropy inequality (3.2) follows as the matrix $\widehat{\mathcal{R}}$ is symmetric positive definite. □

The scheme (3.1) is an ESPC scheme.

3.1. Choice of the numerical viscosity operator. Entropy stability holds for any choice of the matrix $\widehat{\mathcal{R}}$ in (3.1) as long as it is symmetric positive definite. As stated before, we aim to find a suitable numerical viscosity that matches the underlying viscous mechanisms. We do so by setting

$$(3.3) \qquad \widehat{\mathcal{R}} = \mathcal{R}\frac{d\mathbf{w}}{d\mathbf{v}},$$

where $\mathcal{R}$ is the viscosity matrix in the parabolic regularization (1.5) of the nonconservative system (1.1) and $\frac{d\mathbf{w}}{d\mathbf{v}}$ is the Jacobian of $\mathbf{w}(\mathbf{v})$. In doing so, we implicitly assume that the matrix $\mathcal{R}\frac{d\mathbf{w}}{d\mathbf{v}}$ is symmetric positive definite. This assumption holds for a large number of nonconservative systems that model physical phenomena. Examples are provided in the next section. Moreover, by using the Jacobian $\frac{d\mathbf{w}}{d\mathbf{v}}(\mathbf{v})$, we are assuming that the mapping $\mathbf{w} \mapsto \mathbf{v}(\mathbf{w}) := \nabla\eta(\mathbf{w})$ is invertible. This is always the case when η is strictly convex.

Observe that setting the numerical viscosity operator as in (3.3) ensures that the equivalent equation for the scheme (3.1) matches (1.5) to leading order.

4. Examples and numerical experiments. We will show that the entropy stable schemes (3.1), with numerical viscosity chosen to match the underlying physical viscosity, improve the approximation to the physically relevant solutions of the nonconservative hyperbolic system (1.1). We consider the following examples.

4.1. Example 1: Coupled Burgers equation. In [4], the authors proposed the following model problem for nonconservative hyperbolic systems:

$$(4.1) \qquad \begin{aligned} \partial_t u + u\,\partial_x(u+v) &= 0, \\ \partial_t v + v\,\partial_x(u+v) &= 0. \end{aligned}$$

The system can be rewritten in the form (1.1) with

$$\mathbf{w} = \begin{bmatrix} u \\ v \end{bmatrix}, \qquad A(\mathbf{w}) = \begin{bmatrix} u & u \\ v & v \end{bmatrix}.$$

If the component equations of this system are added, then the Burgers equation for $w := u + v$ is obtained:

$$\partial_t w + \partial_x\left(\frac{w^2}{2}\right) = 0.$$

Therefore, (4.1) is termed the *coupled Burgers system*. The Burgers equation satisfied by the sum $w = u + v$ suggests the following entropy pair:

$$\eta(\mathbf{w}) = \frac{w^2}{2}, \qquad q(\mathbf{w}) = \frac{w^3}{3}.$$

In [2], Berthon computed the exact viscous profile of the regularized system

$$(4.2) \qquad \begin{aligned} \partial_t u + u\,\partial_x(u+v) &= \varepsilon_1 \partial_{xx}^2(u+v), \\ \partial_t v + v\,\partial_x(u+v) &= \varepsilon_2 \partial_{xx}^2(u+v). \end{aligned}$$

In the limit $\varepsilon_1, \varepsilon_2 \to 0$ this gives the correct (physically relevant) entropy solution of the Riemann problem for the coupled Burgers equation. In what follows we choose $\varepsilon_1 = \varepsilon_2 = \varepsilon$.

4.1.1. Godunov method. A path consistent scheme can be derived by computing the exact solutions of the Riemann problems at the interfaces and averaging these solutions at the next time level under the appropriate CFL condition. Following [16], the Godunov method can also be interpreted as a path consistent method (1.11) with

$$\mathbf{D}_{i+^1/_2}^- = \int_0^1 A(\Phi(s; \mathbf{w}_i^n, \mathbf{w}_{i+1/2}^{n,-}))\partial_s \Phi(s; \mathbf{w}_i^n, \mathbf{w}_{i+1/2}^{n,-})\,ds,$$

$$\mathbf{D}_{i+^1/_2}^+ = \int_0^1 A(\Phi(s; \mathbf{w}_{i+1/2}^{n,+}, \mathbf{w}_{i+1}^n))\partial_s \Phi(s; \mathbf{w}_{i+1/2}^{n,+}, \mathbf{w}_{i+1}^n)\,ds,$$

where $\mathbf{w}_{i+^1/_2}^{n,\pm}$ are the limits to the left and to the right of $x = 0$ of the solution of the Riemann problem with initial data $(\mathbf{w}_i^n, \mathbf{w}_{i+1}^n)$.

To test the performance of the Godunov scheme, we approximate the Riemann problem for (4.1) with initial data $\mathbf{w}_l = [7.99, 11.01]^\top$, $\mathbf{w}_r = [0.25, 0.75]^\top$ and compare the exact solution with the numerical one provided by the Godunov method in the interval $[-2, 10.5]$ with 1500 points and CFL $= 0.4$. As shown in Figure 1.1, the location of the discontinuities is correctly approximated, whereas the intermediate states approximated by the Godunov scheme are incorrect. The error in these intermediate states does vanish as Δx tends to 0.

This numerical result is rather disheartening. Even though the Godunov method takes into account the exact expression of the viscous profiles (paths) and the exact solutions of the Riemann problems, the numerical solutions provided by the method do not converge to the expected weak solutions due to the numerical viscosity added in the projection step.

4.1.2. ECPC and ESPC schemes. Next, we derive the entropy conservative (ECPC) and entropy stable (ESPC) schemes for the coupled Burgers system.

Let $w = u + v$ be the sum of the unknowns in (4.1). We consider the entropy function $\eta(w) = \frac{w^2}{2}$ with corresponding entropy flux $q(w) = \frac{w^3}{3}$. The entropy variables are $\mathbf{v} = [w, w]^\top$.

To compute the corresponding ECPC scheme, we have to derive fluctuations that satisfy (2.1). Inserting into (2.1) and using (1.11b), we get

$$
\begin{aligned}
0 &\overset{!}{=} \mathbf{v}_i^\top \mathbf{D}_{i+1/2}^- + \mathbf{v}_{i+1}^\top \mathbf{D}_{i+1/2}^+ - [\![q]\!]_{i+1/2} \\
&= \mathbf{v}_i^\top \left(\int_0^1 A(\Phi) \partial_s \Phi ds - \mathbf{D}_{i+1/2}^+ \right) + \mathbf{v}_{i+1}^\top \mathbf{D}_{i+1/2}^+ - \left[\!\!\left[\tfrac{w^3}{3} \right]\!\!\right]_{i+1/2} \\
&= [\![\mathbf{v}]\!]_{i+1/2}^\top \mathbf{D}_{i+1/2}^+ + \mathbf{v}_i^\top \int_0^1 A(\Phi) \partial_s \Phi ds - \left[\!\!\left[\tfrac{w^3}{3} \right]\!\!\right]_{i+1/2} \\
&= [\![w]\!]_{i+1/2} \left(D_{1,i+1/2}^+ + D_{2,i+1/2}^+ \right) + w_i \left(\int_0^1 \Phi_u \Phi_v' ds + \int_0^1 \Phi_u' \Phi_v ds \right) - \left[\!\!\left[\tfrac{w^3}{3} \right]\!\!\right]_{i+1/2},
\end{aligned}
$$

where $\Phi = [\Phi_u(s; \mathbf{w}_i, \mathbf{w}_{i+1}), \Phi_v(s; \mathbf{w}_i, \mathbf{w}_{i+1})]^\top$ is any family of paths and $\mathbf{D}_{i+1/2}^\pm = [D_{1,i+1/2}^\pm, D_{2,i+1/2}^\pm]^\top$. Hence,

$$
\begin{aligned}
D_{1,i+1/2}^+ + D_{2,i+1/2}^+ &= \frac{1}{[\![w]\!]_{i+1/2}} \left(\left[\!\!\left[\tfrac{w^3}{3} \right]\!\!\right]_{i+1/2} - w_i \left(\int_0^1 \Phi_u \Phi_v' ds + \int_0^1 \Phi_u' \Phi_v ds \right) \right) \\
&= \frac{1}{[\![w]\!]_{i+1/2}} \left(\left[\!\!\left[\tfrac{w^3}{3} \right]\!\!\right]_{i+1/2} - w_i \int_0^1 (\Phi_u \Phi_v)' ds \right) \\
&= \frac{1}{6} [\![w]\!]_{i+1/2} \left(w_i + 2w_{i+1} \right).
\end{aligned}
$$

Likewise, we can solve for $\mathbf{D}_{i+1/2}^-$ and obtain

$$
D_{1,i+1/2}^- + D_{2,i+1/2}^- = \frac{1}{6} [\![w]\!]_{i+1/2} \left(2w_i + w_{i+1} \right).
$$

There are infinitely many choices of the two components of $\mathbf{D}_{i+1/2}^-$ and $\mathbf{D}_{i+1/2}^+$. Requiring symmetry and similarity with (4.1), we obtain the following scheme:

$$
\begin{aligned}
\mathbf{D}_{i+1/2}^- &= \frac{1}{6} [\![w]\!]_{i+1/2} \begin{bmatrix} 2u_i + u_{i+1} \\ 2v_i + v_{i+1} \end{bmatrix} + \frac{1}{2} \begin{bmatrix} \int \Phi_u \Phi_v' - \overline{u}_{i+1/2} [\![v]\!]_{i+1/2} \\ \int \Phi_u' \Phi_v - [\![u]\!]_{i+1/2} \overline{v}_{i+1/2} \end{bmatrix}, \\
\mathbf{D}_{i+1/2}^+ &= \frac{1}{6} [\![w]\!]_{i+1/2} \begin{bmatrix} u_i + 2u_{i+1} \\ v_i + 2v_{i+1} \end{bmatrix} + \frac{1}{2} \begin{bmatrix} \int \Phi_u \Phi_v' - \overline{u}_{i+1/2} [\![v]\!]_{i+1/2} \\ \int \Phi_u' \Phi_v - [\![u]\!]_{i+1/2} \overline{v}_{i+1/2} \end{bmatrix}.
\end{aligned}
$$

If the family of straight line segments is chosen, then $\int \Phi_u \Phi_v' = \overline{u}[\![v]\!]$ and $\int \Phi_u' \Phi_v = [\![u]\!]\overline{v}$, so the above reduces to

$$
(4.3) \qquad \mathbf{D}_{i+1/2}^- = \frac{1}{6} [\![w]\!]_{i+1/2} \begin{bmatrix} 2u_i + u_{i+1} \\ 2v_i + v_{i+1} \end{bmatrix}, \qquad \mathbf{D}_{i+1/2}^+ = \frac{1}{6} [\![w]\!]_{i+1/2} \begin{bmatrix} u_i + 2u_{i+1} \\ v_i + 2v_{i+1} \end{bmatrix}.
$$

We derive an ESPC scheme by using a standard central difference to approximate the viscous operator $\varepsilon(u+v)_{xx}$ in the parabolic regularization (4.2):

$$\varepsilon \frac{w_{i-1} - 2w_i + w_{i+1}}{\Delta x^2}.$$

The modified fluctuation functions are then

(4.4)
$$\widetilde{\mathbf{D}}_{i+1/2}^- = \frac{1}{6}[\![w]\!]_{i+1/2} \begin{bmatrix} 2u_i + u_{i+1} \\ 2v_i + v_{i+1} \end{bmatrix} - \frac{\varepsilon}{\Delta x} \begin{bmatrix} [\![w]\!]_{i+1/2} \\ [\![w]\!]_{i+1/2} \end{bmatrix},$$

$$\widetilde{\mathbf{D}}_{i+1/2}^+ = \frac{1}{6}[\![w]\!]_{i+1/2} \begin{bmatrix} u_i + 2u_{i+1} \\ v_i + 2v_{i+1} \end{bmatrix} + \frac{\varepsilon}{\Delta x} \begin{bmatrix} [\![w]\!]_{i+1/2} \\ [\![w]\!]_{i+1/2} \end{bmatrix}.$$

LEMMA 4.1. *The scheme* (1.9) *with fluctuations* (4.4) *is an ESPC scheme for the coupled Burgers system* (4.1)*, that is, it is entropy stable with respect to the entropy* $\eta(\mathbf{w}) = \frac{(u+v)^2}{2}$ *and is path consistent with the family of straight line segments.*

Proof. The scheme is path consistent by construction. The numerical viscosity matrix for (4.4) is $\widehat{\mathcal{R}} = \frac{1}{2}\mathbf{I}$, so entropy stability follows from Theorem 3.1(ii). □

As the scheme (1.9) is semidiscrete, we perform the time integration using a forward Euler method. The time step Δt has to satisfy the CFL condition

$$\Delta t \left(\max_i \frac{|\lambda_i|}{\Delta x} + \frac{2\varepsilon}{\Delta x^2} \right) \le 1,$$

where $\lambda_i = u_i + v_i$. We select a CFL number of 0.4 in what follows. Furthermore, we choose $\varepsilon = 4\Delta x$ in our computations.

In order to validate the ESPC scheme, we consider again the Riemann problem with initial data $\mathbf{w}_l = [7.99, 11.01]^\top$, $\mathbf{w}_r = [0.25, 0.75]^\top$ and compare the exact solution with the numerical one provided by the ESPC scheme in the interval $[-2, 10.5]$ with 1500 grid points. The results are shown in Figure 4.1. In order to compare the ESPC scheme with the Godunov scheme, we computed the numerical Hugoniot locus by approximating a family of Riemann problems whose initial data are given by $\mathbf{w}_r = [0.75, 0.25]^\top$ and a series of left states belonging to the exact shock curve. The Riemann problem is solved in the interval $[-2, 10]$ and the corresponding left state (at the shock) is used to compute the numerical Hugoniot locus. The results are
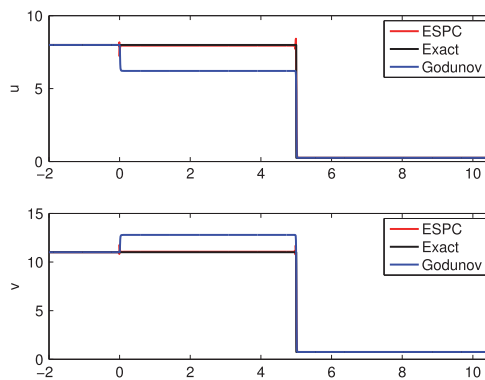

FIG. 4.1. *Comparison of the ESPC and Godunov schemes for the coupled Burgers system* (4.1) *with the exact solution.*
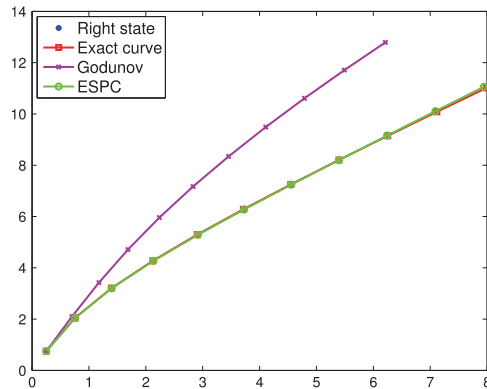
FIG. 4.2. *The numerical Hugoniot locus for the coupled Burgers equation* (4.1) *determined from the approximate solutions generated by the ESPC and Godunov schemes, compared with an exact Hugoniot locus.*

presented in Figure 4.2 and show that the Godunov scheme does a poor job of approximating the exact solution. The numerical Hugoniot locus for this scheme starts diverging even for shocks with small amplitude. On the other hand, the ESPC scheme approximates the correct weak solution. The numerical Hugoniot locus coincides with the exact locus for a large range of shock strengths. Only for very strong shocks does the Hugoniot locus show a slight deviation. This is to be expected as the high-order terms in the equivalent equation (1.12) become larger with increasing shock strength and may lead to deviations in the computed solution. However, the gain in accuracy with the ESPC scheme over the Godunov scheme is considerable.

Remark 4.2. The ESPC scheme for the coupled Burgers equation is path consistent with a family of straight line segments, yet it accurately approximates the exact solutions that are based on a path computed from the viscous profile. This example indicates that the choice of paths is not crucial in determining which solutions are approximated by the scheme. Instead, the numerical viscosity operator (that matches with the underlying viscosity) decides which weak solution the scheme will converge to.

4.2. Example 2: Two-layer shallow water equations. We consider the system of partial differential equations governing the one-dimensional flow of two superposed immiscible shallow layers of fluids:

$$(h_1)_t + (h_1 u_1)_x = 0,$$
$$(h_2)_t + (h_2 u_2)_x = 0,$$
(4.5)
$$(h_1 u_1)_t + \left(\frac{1}{2}g h_1^2 + h_1 u_1^2\right) = -g h_1 (b + h_2)_x,$$
$$(h_2 u_2)_t + \left(\frac{1}{2}g h_2^2 + h_2 u_2^2\right) = -g h_2 (b + r h_1)_x.$$

Here, $u_j(x,t)$ and $h_j(x,t)$ represent respectively the depth-averaged velocity and the thickness of the jth layer, g is acceleration due to gravity, and $b = b(x)$ is the bottom topography. In these equations, indexes 1 and 2 refer to the upper and lower layers. Each layer is assumed to have a constant density ρ_j ($\rho_1 < \rho_2$), and $r = \rho_1/\rho_2$ is the density ratio.

The underlying viscous mechanism is the eddy viscosity, leading to the mixed hyperbolic-parabolic system (see [14]):

$$(h_1)_t + (h_1 u_1)_x = 0,$$
$$(h_2)_t + (h_2 u_2)_x = 0,$$

(4.6)
$$(h_1 u_1)_t + \left(\frac{1}{2}gh_1^2 + h_1 u_1^2\right) = -gh_1(b + h_2)_x + \nu(h_1(u_1)_x)_x,$$

$$(h_2 u_2)_t + \left(\frac{1}{2}gh_2^2 + h_2 u_2^2\right) = -gh_2(b + rh_1)_x + \nu(h_2(u_2)_x)_x.$$

Here, $\nu \ll 1$ is the coefficient of eddy viscosity. An entropy-entropy flux pair for the two-layer shallow water system is given by

(4.7a)
$$\eta(\mathbf{w}) = \sum_{j=1}^{2} \rho_j \left(h_j \frac{u_j^2}{2} + g\frac{h_j^2}{2} + gh_j b \right) + g\rho_1 h_1 h_2,$$

(4.7b)
$$q(\mathbf{w}) = \sum_{j=1}^{2} \rho_j \left(h_j \frac{u_j^2}{2} + gh_j^2 + gh_j b \right) u_j + \rho_1 gh_1 h_2 (u_1 + u_2).$$

The corresponding entropy variables are

$$\mathbf{v} = \begin{bmatrix} \rho_1 \left(-\frac{1}{2}u_1^2 + g(h_1 + h_2 + b) \right) \\ \rho_1 u_1 \\ \rho_2 \left(-\frac{1}{2}u_2^2 + g(h_2 + b) \right) + \rho_1 gh_1 \\ \rho_2 u_2 \\ \rho_1 gh_1 + \rho_2 gh_2 \end{bmatrix}.$$

In a recent paper [9], the following scheme has been presented:

(4.8) $\dfrac{d}{dt}\mathbf{u}_i + \dfrac{1}{\Delta x}\left(\mathbf{F}_{i+1/2} - \mathbf{F}_{i-1/2}\right) + \dfrac{1}{\Delta x}\left(B_{i+1/2}^- + B_{i-1/2}^+\right) = \dfrac{1}{\Delta x}\left(\mathbf{S}_{i+1/2}^- + \mathbf{S}_{i-1/2}^+\right),$

where

$$\mathbf{F}_{i+1/2} = \begin{bmatrix} \overline{(h_1)}_{i+1/2}\overline{(u_1)}_{i+1/2} \\ \frac{1}{2}g\overline{(h_1^2)}_{i+1/2} + \overline{(h_1)}_{i+1/2}\overline{(u_1)}_{i+1/2}^2 \\ \overline{(h_2)}_{i+1/2}\overline{(u_2)}_{i+1/2} \\ \frac{1}{2}g\overline{(h_2^2)}_{i+1/2} + \overline{(h_2)}_{i+1/2}\overline{(u_2)}_{i+1/2}^2 \end{bmatrix},$$

$$B_{i+1/2}^\pm = \begin{bmatrix} 0 \\ \frac{g}{2}\overline{(h_1)}_{i+1/2}[\![h_2]\!]_{i+1/2} \\ 0 \\ \frac{gr}{2}\overline{(h_2)}_{i+1/2}[\![h_1]\!]_{i+1/2} \end{bmatrix}, \quad \mathbf{S}_{i+1/2}^\pm = \begin{bmatrix} 0 \\ -\frac{g}{2}\overline{(h_1)}_{i+1/2}[\![b]\!]_{i+1/2} \\ 0 \\ -\frac{g}{2}\overline{(h_2)}_{i+1/2}[\![b]\!]_{i+1/2} \end{bmatrix}.$$

Here,

$$\overline{a}_{i+1/2} = \frac{a_i + a_{i+1}}{2}.$$

It is straightforward to write down the above scheme in the fluctuation form (1.9) and check that the scheme (4.8) is an ECPC scheme with respect to (η, q) and the straight line segment paths.

To derive an ESPC scheme, we discretize the eddy viscosity by using a centered approximation:

(4.9)
$$\nu \left(h_j(u_{j,x})\right)_x\big|_{x=x_i} \approx \frac{\nu}{\Delta x^2}\left(\overline{(h_j)}_{i+1/2}[\![(u_j)]\!]_{i+1/2} - \overline{(h_j)}_{i-1/2}[\![(u_j)]\!]_{i-1/2}\right), \quad j=1,2.$$

By multiplying the resulting scheme by $\mathbf{v}_i$, as in the proof of Theorem 3.1, we find that the scheme is entropy stable.

The following numerical schemes are compared here:

- The ESPC scheme with numerical viscosity given by the discretization (4.9) of the eddy viscosity with $\nu = C\Delta x$.
- As the eddy viscosity does not act on the mass equations, some oscillations may appear on the numerical solutions. Therefore, we also consider a modified ESPC scheme where some viscosity is added to the mass conservation equations:

$$\varepsilon\,(h_j)_{xx}\big|_{x=x_i} \approx \frac{C}{\Delta x^2}\left([\![h_j]\!]_{i+1/2} - [\![h_j]\!]_{i-1/2}\right), \qquad j=1,2.$$

This scheme with eddy viscosity as well the numerical viscosity in the mass equations is called the ESPC-NV scheme. We set $C = \nu/10$ in the numerical experiments.

- The Roe scheme consistent with the straight line paths of [4], [19].
- The central upwind (CU) scheme of Kurganov and Petrova [12].

Notice that only for the first of these three methods, the numerical viscosity agrees with the physical eddy viscosity to leading order.

It is very difficult to compute the viscous profiles explicitly from the viscous shallow water system (4.6). Instead, we compute the reference solutions by taking a fixed $\nu \ll 1$ in the ESPC scheme, computed on very fine meshes.

In Figure 4.3, we plot the solutions obtained with the ESPC, ESPC-NV, and Roe schemes for a Riemann problem with initial data

(4.10)
$$\mathbf{w}_l = \begin{bmatrix} 1.376 \\ 0.6035 \\ 0.04019 \\ -0.04906 \end{bmatrix}, \qquad \mathbf{w}_r = \begin{bmatrix} 0.37 \\ 1.593 \\ -0.1868 \\ 0.1742 \end{bmatrix}$$
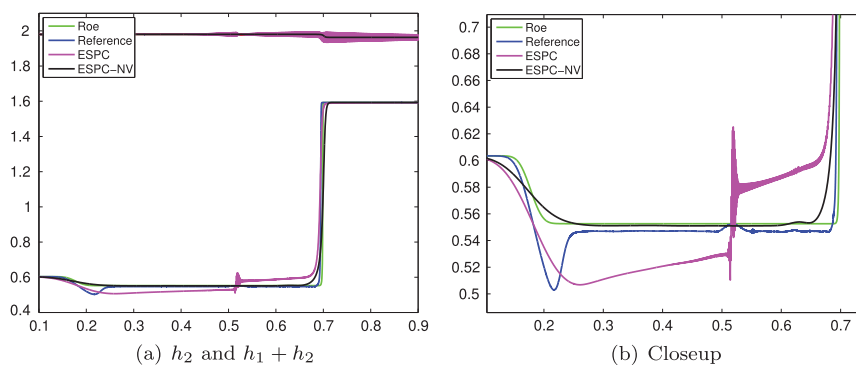

(a) h_2 and $h_1 + h_2$

(b) Closeup

FIG. 4.3. *Approximate solutions for height of bottom layer (h_2) and total height (h_1+h_2) for the two-layer shallow water system (4.5) with the ESPC, ESPC-NV, and path consistent Roe schemes. A reference solution, computed from the viscous shallow water system (4.6), is also displayed.*
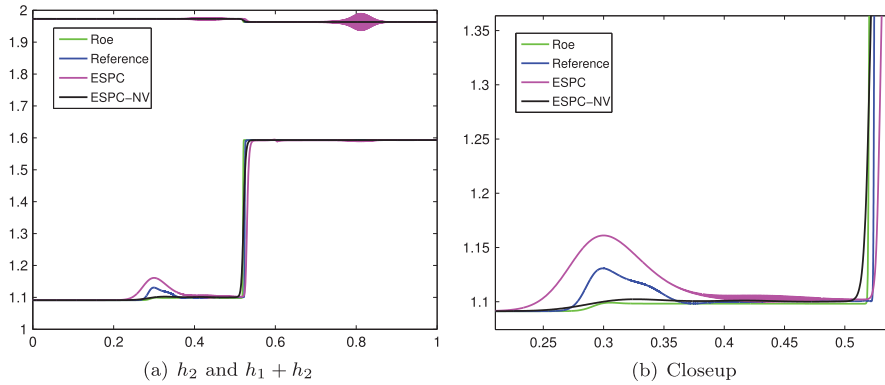
(a) h_2 and $h_1 + h_2$

(b) Closeup

FIG. 4.4. *Similar to Figure* 4.3, *but with initial data* (4.11).

and homogeneous Neumann boundary conditions on the computational domain $[0, 1]$. The ratio of densities is set to $r = 0.98$ and $g = 9.81$. All the simulations are performed with 2000 mesh points. The reference solution is computed on a very fine mesh of 2^{16} mesh points with $\nu = 2 \times 10^{-4}$. As seen in Figure 4.3, the solutions computed with all the schemes are quite close to the reference solution. As seen in the closeup, there is a minor difference in the intermediate state computed by the ESPC-NV and Roe schemes. The ESPC scheme contains oscillations. This is to be expected as the mass conservation equations contain no numerical viscosity. However, the approximate solution computed by this scheme is still quite close to the reference solution.

In Figure 4.4 we show the solutions obtained with the same numerical schemes for a Riemann problem with initial data

$$(4.11) \qquad \mathbf{w}_l = \begin{bmatrix} 0.8817 \\ 1.091 \\ -0.1738 \\ 0.1613 \end{bmatrix}, \qquad \mathbf{w}_r = \begin{bmatrix} 0.37 \\ 1.593 \\ -0.1868 \\ 0.1742 \end{bmatrix}.$$

Notice that the right state is the same as in (4.10), but the left state is closer, resulting in a smaller shock. Again, the computed shock speed and intermediate states computed with ESPC, ESPC-NV, and Roe are quite close.

This is not the case for the CU scheme. The derivation of this scheme is based on the following assumption: as in the geophysical applications, in which the density ratio is close to one, the surface waves are much smaller that the internal ones, if the vertical coordinate z is chosen so that $z = 0$ corresponds to the free surface of the undisturbed water, then $\varepsilon_f = h_1 + h_2 + b \approx 0$. Therefore, if the equations are rewritten so that the nonconservative products have the form $\varepsilon_f \partial_x h_i$, the authors of [12] expect that these products could be negligible at the intercells. In the case of the Riemann problem with initial data (4.11) with a flat bottom there is more than one possible choice for the undisturbed water level: one can decide that this level corresponds to the initial surface of the left state (which corresponds to the choice $b = -h_{1,l} - h_{2,l}$), to the right state ($b = -h_{1,r} - h_{2,r}$), or to the average ($b = -0.5(h_{1,l} + h_{2,l} + h_{1,r} + h_{2,4})$), among many other possible choices. The variation of the initial value of ε_f corresponding to these three possible choices is less than 1%. And, of course, the exact solution is not expected to depend on the particular
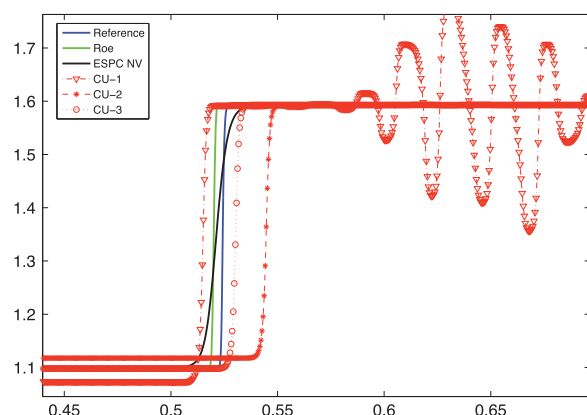
FIG. 4.5. *Approximate solutions for the height of bottom layer (h_2) computed with ESPC-NV, path consistent Roe, and CU schemes for initial data* (4.11) *using different total water levels.*

choice of b as, in this case, it is constant and it only appears in the equations through its derivative. In Figure 4.5 we show the solutions obtained with ESPC-NV, Roe, and CU schemes for the Riemann problem with initial condition (4.11) and the three different choices of b. While ESPC-NV and Roe schemes always provide the same solution, as expected, this is not the case for the CU scheme: notice the strong differences between the computed numerical solutions depending on the choice of b including the appearance of numerical oscillations. Similar results are obtained if the Riemann problem (4.10) is considered. Moreover, the differences between the numerical solutions provided by the CU scheme may be considerably enlarged by increasing the ratio of densities. These numerical tests seem to indicate that the fact of neglecting $\varepsilon_f \partial_x h_i$ at intercells as in [12] may lead to unphysical solutions.

In order to compare the performance of the schemes (the CU scheme is not considered) for a large set of initial data, we compute a *numerical* Hugoniot locus by fixing the same right state as in (4.10) and then varying the left state. In this experiment $r = 0.98$ and $g = 9.81$. A reference Hugoniot locus is calculated by using again the ESPC scheme with $\nu = 2 \times 10^{-4}$ and a mesh of 2^{16} points. The corresponding Hugoniot locus are labeled *Reference* in Figure 4.6. In order to illustrate the dependence of the weak solutions of the two-layer shallow water equations on the choice of paths, we choose an alternative path by fixing a left state $\mathbf{w}_l$ and computing numerically the states that can be linked to this state by a shock satisfying the Rankine–Hugoniot conditions associated to the family of straight line segments, that is,

$$(4.12) \quad \begin{cases} \sigma[\![h_1]\!] = [\![h_1 u_1]\!], \\ \sigma[\![h_1 u_1]\!] = \left[\!\left[\frac{1}{2}gh_1^2 + h_1 u_1^2\right]\!\right] + g\overline{h_1}[\![h_2]\!], \\ \sigma[\![h_2]\!] = [\![h_2 u_2]\!], \\ \sigma[\![h_2 u_2]\!] = \left[\!\left[\frac{1}{2}gh_2^2 + h_2 u_2^2\right]\!\right] + gr\overline{h_2}[\![h_2]\!]. \end{cases}$$

To calculate this curve, σ is taken as a parameter and the nonlinear system (4.12) is numerically solved to obtain the value of $\mathbf{w}_r$; see [3] for details. The computed Hugoniot locus is labeled *Segments* in Figure 4.6. The Hugoniot loci computed with the three numerical schemes in the h_1-$(h_1 u_1)$ plane and the h_2-$(h_2 u_2)$ plane are also shown in Figure 4.6.

From Figure 4.6, we observe that the Hugoniot locus calculated using straight line segments is clearly different from the one calculated from the underlying viscous
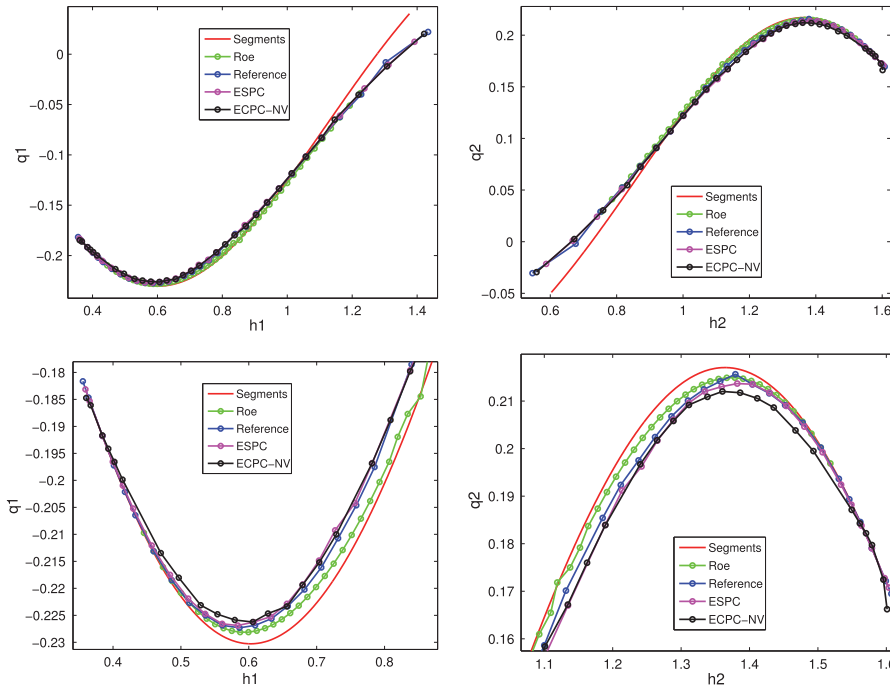
FIG. 4.6. *Hugoniot loci in the h_1-(h_1u_1) and h_2-(h_2u_2) planes for the two-layer shallow water equations* (4.5), *computed with the ESPC, ESPC-NV, and Roe schemes. A reference Hugoniot locus computed from the viscous shallow water system* (4.6) *and a Hugoniot locus computed using straight line paths from* (4.12) *are also shown.*

two-layer shallow water equations (4.6). On the other hand, all three numerical schemes lead to Hugoniot loci that are very close to each other and to the reference Hugoniot locus. Minor differences are visible when we zoom in; see the bottom row of Figure 4.6. We see that among the three schemes, the ESPC scheme provides the best overall approximation to the reference Hugoniot locus. However, both the ESPC-NV and Roe schemes also provide a good approximation to the reference Hugoniot locus. The results show that (rather surprisingly) the numerical approximation of two-layer shallow water equations is not as sensitive to the viscous terms as the coupled Burgers system. The path consistent Roe scheme performs adequately in approximating the correct solution. At the same time, the ESPC schemes proposed in this paper provide a slightly more accurate approximation.

5. Conclusion. This paper deals with accurate numerical approximation of the nonconservative hyperbolic system (1.1). We need to interpret a product of distributions in order to define weak solutions for this nonconservative system. The concept of paths, based on the theory of [5], can be used to define this nonconservative product. Consequently, the definition of weak solutions depends on the choice of paths and different paths can lead to different weak solutions. Furthermore, solutions of the nonconservative system (1.1) depend *explicitly* on underlying small-scale mechanism like diffusion. Hence, the physically relevant solutions of (1.1) can be realized as the limit of the underlying mixed hyperbolic-parabolic system (1.5).

This explicit dependence of the solutions on the underlying viscous mechanisms has profound implications on the design of numerical schemes. In particular, numerical approximations of nonconservative systems, including the family of path consistent

numerical schemes designed in [18], may fail to converge to the physically relevant solution. This observed lack of convergence is due to the (implicit) numerical viscosity added by these schemes being different from the underlying physical viscosity in (1.5).

We address this issue in the current paper by designing finite difference schemes based on two ingredients. First, we extend the notion of entropy conservative schemes, introduced for conservative hyperbolic systems in [20], to nonconservative hyperbolic systems by designing ECPC schemes. The ECPC schemes do not contain any numerical viscosity (at leading order). The second ingredient of our framework is to add numerical viscosity operators that match the underlying physical viscosity in (1.5). The resulting schemes are shown to be entropy stable. The equivalent equation of these schemes agrees with the underlying viscous system (1.5) to leading order. Hence, these ESPC schemes are expected to converge to the physically relevant solutions of (1.1), at least for shocks with small amplitude.

The performance of ESPC schemes is illustrated by presenting numerical results for two model systems: the coupled Burgers system (4.1) and the two-layer shallow water system (4.5). We see that the ESPC schemes approximate the physically relevant solutions quite well in both cases. Furthermore, the ESPC schemes are quite simple to implement.

The main principle underlying the design of ESPC schemes is the agreement between the equivalent equation of the scheme and the underlying parabolic system (1.5). This equivalence holds as long as the residual terms in the equivalent equation are small. However, for shocks of large amplitude, these residual terms might be significant and the scheme might fail to converge to the correct solution. We will describe very-high-order numerical schemes that provide a remedy for this situation in a forthcoming paper.

REFERENCES

[1] R. ABGRALL AND S. KARNI, *A comment on the computation of non-conservative products,* J. Comput. Phys., 45 (2010), pp. 382–403.

[2] C. BERTHON, *Nonlinear scheme for approximating a non-conservative hyperbolic system,* C. R. Math. Acad. Sci. Paris, 335 (2002), pp. 1069–1072.

[3] M. J. CASTRO, P. G. LEFLOCH, M. L. MUÑOZ, AND C. PARÉS, *Why many theories of shock waves are necessary: Convergence error in formally path-consistent schemes,* J. Comput. Phys., 227 (2008), pp. 8107–8129.

[4] M. J. CASTRO, J. MACÍAS, AND C. PARÉS, *A Q-scheme for a class of systems of coupled conservation laws with source term. Application to a two-layer 1-D shallow water system,* M2AN Math. Model. Numer. Anal., 35 (2001), pp. 107–127.

[5] G. DAL MASO, P. G. LEFLOCH, AND F. MURAT, *Definition and weak stability of non-conservative products,* J. Math. Pures Appl., 74 (1995), pp. 483–548.

[6] U. S. FJORDHOLM AND S. MISHRA, *Accurate Numerical Discretizations of Non-Conservative Hyperbolic Systems,* Research report 2010–25, Seminar für Angewandte Mathmatik, ETH Zürich, 2010.

[7] U. S. FJORDHOLM, S. MISHRA, AND E. TADMOR, *Energy preserving and energy stable schemes for the shallow water equations,* in Foundations of Computational Mathematics, London Math. Soc. Lecture Note Ser., 2009, pp. 93–139.

[8] U. S. FJORDHOLM, S. MISHRA, AND E. TADMOR, *Well-balanced and energy stable schemes for the shallow water equations with discontinuous topography,* J. Comput. Phys., 230 (2011), pp. 5587–5609.

[9] U. S. FJORDHOLM, *Energy Conservative and -Stable Schemes for the Two-Layer Shallow Water Equations,* Technical report, Seminar for Applied Mathematics, ETH Zurich, 2010.

[10] T. Y. HOU AND P. G. LEFLOCH, *Why non-conservative schemes converge to wrong solutions: Error analysis,* Math. Comp., 62 (1994), pp. 497–530.

[11] S. KARNI, *Viscous shock profiles and primitive formulations,* SIAM J. Numer. Anal., 29 (1992), pp. 1592–1609.

[12] A. KURGANOV AND G. PETROVA, *Central-upwind schemes for two-layer shallow water equations,* SIAM J. Sci. Comput., 31 (2009), pp. 1742–1773

[13] R. J. LeVEQUE, *Finite Volume Methods for Hyperbolic Problems,* Cambridge University Press, Cambridge, UK, 2002.

[14] G. NARBONA-REINA, J. D. D. ZABSONRÉ, E. D. FERNÁNDEZ-NIETO, AND D. BRESCH, *Derivation of a bilayer model for shallow water equations with viscosity. Numerical validation,* CMES Comput. Model. Eng. Sci., 43 (2009), pp. 27–71.

[15] M. L. MUÑOZ AND C. PARÉS, *On some difficulties of the numerical approximation of nonconservative hyperbolic systems,* Bol. Soc. Esp. Mat. Apl., 47 (2009), pp. 23–52.

[16] M. L. MUÑOZ AND C. PARÉS, *Godunov method for non-conservative hyperbolic systems,* Math. Model. Numer. Anal., 41 (2007), pp. 169–185.

[17] M. L. MUÑOZ AND C. PARÉS, *On the convergence and well-balanced property of path-conservative numerical schemes for systems of balance laws,* J. Sci. Comput. 48 (2011), pp. 274–295.

[18] C. PARÉS, *Numerical methods for non-conservative hyperbolic systems: A theoretical framework,* SIAM J. Numer. Anal., 44 (2006), pp. 300–321.

[19] C. PARÉS AND M. J. CASTRO, *On the well-balanced property of Roe's method for non-conservative hyperbolic systems. Applications to shallow-water systems,* Math. Model. Numer. Anal., 38 (2004), pp. 821–852.

[20] E. TADMOR, *The numerical viscosity of entropy stable schemes for systems of conservation laws. I,* Math. Comput., 49 (1987), pp. 91–103.